Pergamon

Available online at www.sciencedirect.com
SCIENCE DIRECT®

Cement and Concrete Research 33 (2003) 873–880

CEMENT AND CONCRETE RESEARCH

Experimental investigation of the behavior of variably confined concrete

Kent A. Harries[a,*], Gayatri Kharel[b]

[a]Department of Civil and Environmental Engineering, University of South Carolina, 300 Main Street, Columbia, SC 29208, USA
[b]South Carolina Department of Transportation, Columbia, SC 29201, USA

Received 11 July 2002; accepted 10 December 2002

Abstract

The behavior of concrete subject to variable levels of confining pressure under concentric axial loading is presented. An extensive experimental investigation of this behavior, using FRP-confined concrete cylinders, is used to develop an understanding of the relationships required to accurately model the behavior of concrete subject to passively induced varying levels of confinement. In particular, the relationship between transverse and longitudinal strains—the dilation relationship—is investigated and a model for this behavior, based on the stiffness of the confining materials, is proposed.

Concrete compressive strength is observed to increase with increasing confinement. Axial strain capacity is observed to increase to a greater degree than the compressive strength resulting in a more ductile axial stress–strain behavior for confined concrete as compared to unconfined concrete. The axial stress–strain behavior is also observed to change from parabolic to bilinear as the level of confinement is increased.

Keywords: Compressive strength; Expansion; Mechanical properties; Modeling; Confinement

1. Introduction

In order to accurately model the behavior of reinforced concrete structures, it is necessary to understand the material behavior of the constituent concrete. While the uniaxial unconfined stress versus strain relationship for plain concrete is well established [1–3], most in situ concrete is confined in some manner. Confinement may take the form of conventional internal reinforcing steel or external steel or fiber-reinforced polymer (FRP) composite jackets. Indeed, core concrete, located in the interior of a structural element, is confined simply by the surrounding concrete. Accurate structural modeling therefore requires a sound understanding of the stress–strain behavior of confined concrete.

The axial stress–strain behaviors of unconfined and confined concrete differ significantly. Furthermore, the nature of the confinement provided also significantly affects the concrete behavior. In conventionally reinforced and externally jacketed concrete columns, confining pressure is *passive* in nature. That is, confining pressure is engaged by the transverse dilation of concrete resulting from principal axial strains—the Poisson effect (shown schematically in Fig. 1). There are cases where an initial *active* confining pressure is present, as is the case when an expansive grout is injected between a column and an external jacket. In these cases, however, the active pressure is generally quite small in comparison to the additional passive pressure generated by concrete dilation.

Passive confinement may be *constant* or *variable* through an axial load history. Constant confining pressure is generated in cases where the confining material behaves in a plastic manner. This is typically assumed to be the case where confinement is provided by conventional transverse reinforcing steel. Variable confining pressure is generated when the confining material has an appreciable stiffness. FRP jackets and steel that are still elastic generate variable confining pressures. Variable passive confinement is dependent on the axial and transverse behavior of the concrete, which in turn is dependent on the amount and stiffness of confinement provided.

1.1. Conventional models of the axial stress–strain behavior of confined concrete

Traditionally, models of the behavior of confined concrete are based on an assumption of constant confining pressure. This is a valid assumption assuming that the concrete is being confined by steel that is yielding and therefore may be assumed to be providing a constant confining pressure. This

* Corresponding author. Tel.: +1-803-777-0671; fax: +1-803-777-0670.
E-mail address: harries@sc.edu (K.A. Harries).

0008-8846/02/$ – see front matter © 2002 Elsevier Science Ltd. All rights reserved.
doi:10.1016/S0008-8846(02)01086-4

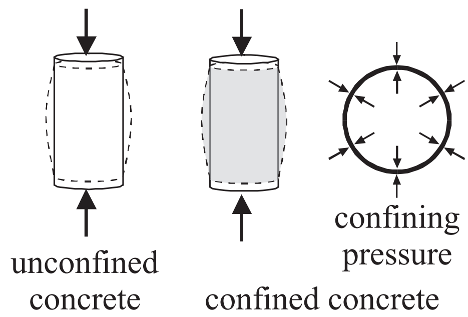

Fig. 1. Confining pressure engaged by dilation of concrete.

is the assumed design criterion for reinforced concrete confined with steel ties or spirals.

Richart et al. [4] first investigated the behavior of concrete in biaxial and triaxial compression by conducting axial compression tests of concrete specimens under hydraulic confining pressure. Richart's model for confined concrete behavior has been empirically modified to reflect additional experimental data [5,6]. Additionally, a number of constitutive models of concrete behavior when subject to biaxial and triaxial loading have been proposed [7–10]. Depending on the nature of the structure, however, simplifying assumptions regarding a suitable concrete model can be made. For most typical cases, a confinement dependent uniaxial model is sufficiently accurate to model the behavior of confined concrete.

For reinforced concrete columns, a number of investigations of large-scale column specimens have been carried out and confined concrete behavior models have been proposed based on the results of these tests [11–14]. The most commonly used model is that proposed by Mander et al. [15] All extant models assume a constant confining pressure generated by the yielding of the confining steel. Fig. 2 shows the predicted confined ultimate concrete compressive stress, f_{cmax}, as a function of the constant confining pressure, f_{con}, provided (both normalized by the compressive strength of unconfined concrete, f_c'). Considerable variability between models is evident reflecting the generally inappropriate assumptions of constant confining pressure and constant dilation ratio used. Also shown in Fig. 2 are the data obtained in this study; these are discussed further below.

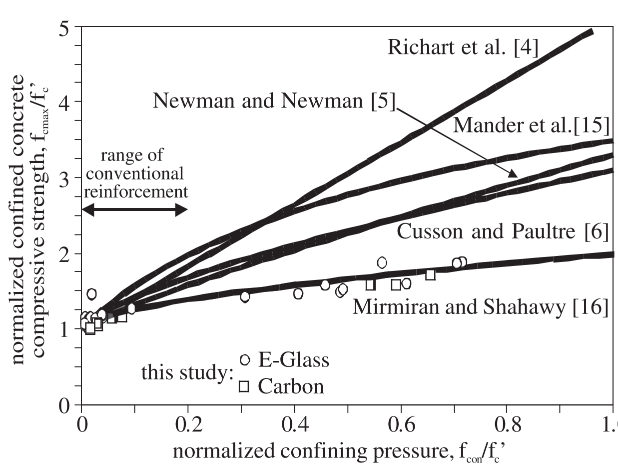

Fig. 2. Maximum compressive strength of confined concrete.

It can be seen from Fig. 2 that a model proposed by Mirmiran and Shahawy [16] very accurately captures the observed experimental responses over a wide range of peak confining pressures. Mirmiran and Shahawy's model, unlike the others shown, accounts for the passive variable nature of confinement provided by external FRP jackets.

Fig. 2 also provides an indication of the level of confining pressure that may be reasonably obtained using external jackets. Conventional transverse steel hoops or spirals are reasonably only able to generate confining pressure up to about $0.2f_c'$. External FRP jackets, on the other hand, may be designed to provide confining pressure upwards of f_c'. The level of confinement will be discussed later.

1.2. Dilation ratio of concrete

To understand the behavior of concrete having variable levels of confinement and to determine the confining pressure generated, the dilation ratio, defined as the ratio of transverse to axial strains, must be clearly defined. The dilation ratio, η, is a generalized interpretation of Poisson's ratio. Poisson's ratio, a constant, may be interpreted as the initial dilation ratio, or the dilation ratio at very low axial strain levels.

The dilation ratio for axially loaded unconfined concrete is typically assumed to have a constant value, equal to Poisson's ratio for concrete, up to an axial stress level of about 70% of the compressive strength of concrete, f_c'. Beyond $0.7f_c'$, the dilation ratio increases rapidly to a value of about 0.5 at f_c' and is unstable in the postpeak response as the concrete dilates in an uncontrolled manner [17]. Elwi and Murray [18] proposed an empirical relationship for the dilation ratio of unconfined concrete as a function of principal axial strain. This proposed relationship, however, is exceptionally unsuited to determining the dilation relationship for confined concrete and does not reflect experimental observations [19]. Fig. 3 shows the concrete dilation ratio

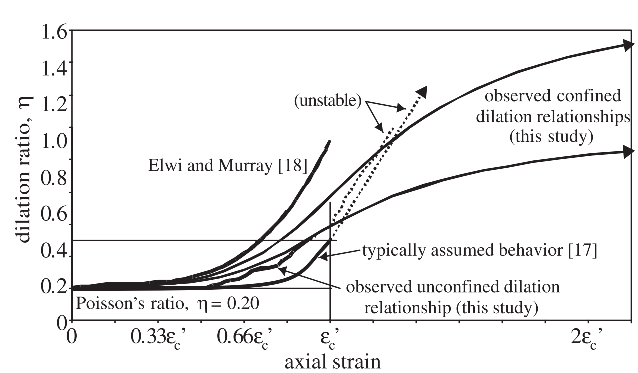

Fig. 3. Proposed and observed dilation behavior of concrete.

versus axial compressive strain relationships for unconfined concrete proposed by Elwi and Murray [18] and by Chen [17]. Also shown in Fig. 3 is an example of the experimentally determined dilation relationship for unconfined concrete found in this study. Fig. 3 also shows examples of the experimentally determined dilation relationship for confined concrete having different levels of confinement. These relationships will be discussed further below. It can be seen that the Elwi and Murray equation does not capture the experimentally determined behavior of unconfined or confined concrete. Furthermore, it is not suitable to apply the dilation relationship for unconfined concrete to the case of confined concrete. An empirical dilation relationship based on confining jacket stiffness developed in this research program is presented below.

In this study, extensive experimental data are introduced to establish empirical relationships necessary to understand the behavior of concrete subject to variable confining pressure. In particular, the relationships between confining pressure and peak concrete response and between axial and transverse strains (the dilation relationship) are established. An iterative, semi-empirical algorithm for modeling the axial stress–strain relationship from variably confined concrete has been presented elsewhere [20].

2. Experimental program

A series of 152-mm diameter by 305-mm tall concrete cylinders were tested [21] using standard test methods [22]. Variable passive confinement was provided by jacketing the cylinders in lightweight glass and carbon materials. The jackets were applied leaving a gap at the top and bottom of the cylinders to ensure that the jackets were not directly subject to axial load. The amount to confinement available (stiffness of jacket) was controlled by the number of plies used to wrap the cylinders.

Lightweight materials were used so that confinement levels (transverse reinforcing ratios) representative of what may be found in real-world applications may be modeled in the smaller-scale test specimens. It is important to note that FRP materials were used in order to generate variable passive confining pressure, as such the jackets should be seen as part of the test setup. This study should not be interpreted as a study of FRP confinement per se.

Table 1 provides jacket material properties for the raw material (manufacturer’s data) and for tensile coupons tested as part of this study. Both materials exhibited a linear response to a sudden rupture failure. Coupon tests corresponding to all tested jacket stiffnesses (plies) were performed, the average values are reported in Table 1. Contrary to previous observations [19], the average jacket strength and stiffness was not significantly affected by the number of plies. It is believed that since the lightweight FRP materials were rather fragile and thus required great care in

Table 1
FRP jacket material properties and test matrix

Parameter	E-Glass	Carbon
Manufacturer’s reported data		
Areal weight	117 g/m^2	97 g/m^2
Strength, $\bar{f}_{fr}$	154 N/mm·ply	350 N/mm·ply
Tensile modulus, $\bar{E}_f$	10.3 kN/mm·ply	25 N/mm·ply
Strain at rupture, ε_{fr}	0.015	0.014
Experimentally determined data		
Strength, $\bar{f}_{fr}$	75 N/mm·ply	174 N/mm·ply
Tensile modulus, $\bar{E}_f$	4.9 kN/mm·ply	15.7 kN/mm·ply
Number of plies tested, n	1, 2, 3, 6, 9, 12, 15	1, 2, 3

handling, superior quality control during the application was achieved. It is further noted that the tensile tests on the FRP materials demonstrated excellent repeatability; a standard deviation no greater than 6% was reported for any test series. The discrepancy between manufacturers’ reported data and experimentally obtained strength and stiffness values are commonly observed [19]. These discrepancies may be partially attributed to quality control and lay-up procedure and partially to in situ effects [19]. These effects are the subject of further work by the author. In the current work, the experimentally obtained values are used as a basis of all calculations and comparisons.

As noted in Table 1, in this study, the FRP jacket material is characterized in terms of strength, $\bar{f}_{fr}$, tensile modulus, $\overline{E}_f$, and strain at rupture ε_{fr}. Strength and modulus are given in units of *force per unit dimension perpendicular to the principle direction of the fibers per ply* (N/mm ply). Such units permit jacket designs to proceed without consideration of the specific jacket material or the final thickness of the jacket. This is particularly useful where hand layed-up material is used since, in such cases, thickness depends on parameters such as fiber volume ratio, fabric geometry, and lay-up technique.

3. Test apparatus and instrumentation

The cylinders were tested in uniaxial compression [22] in a 2225-kN capacity concrete cylinder test machine. Instrumentation recorded the applied axial load, axial and transverse strains and strains on the FRP material itself. At least five cylinders of each material (glass or carbon) and each level of confinement (number of plies) were tested (see Table 1).

All confined cylinders had electrical resistance strain gages located at midheight, oriented perpendicular to the longitudinal axis of the cylinder to measure hoop strain in the jackets. A standard compressometer–extensometer was used to measure the axial and the transverse deformation of the cylinder [22]. Values obtained from this instrument were used in determining the modulus and dilation parameters of the cylinders.

4. Experimental results

Table 2 gives average values of the major parameters measured and the ratios of these parameters to those measured for unconfined concrete. The values presented are averaged over at least five specimens. Fig. 4 shows representative stress versus axial and transverse strain curves for the cylinders tested. Fig. 5 shows the dilation versus axial strain relationships for the cylinders tested. The following conclusions may be drawn from the experimental results presented:

1. Maximum concrete stress, f_{cmax}, increases with an increase in the confinement provided.
2. The strain corresponding to the maximum concrete stress, ε_{cmax}, generally increases with an increase in confinement used. This increase is greater than that exhibited by concrete stress, therefore it may be said that the ductility capacity (measured as the ratio of ultimate deformation to the deformation corresponding to "yield") increases with increased confinement.
3. The initial modulus of the confined and unconfined concrete is similar. The expected decay in modulus (softening of the response) accompanying increased axial strain is reduced when confinement is present.
4. From Fig. 5, it can be seen that dilation ratio varies with axial compressive strain. The observed initial dilation ratio is approximately equal to Poisson's ratio and remains essentially constant through an axial strain of about 0.0018, 60% of the unconfined concrete axial strain corresponding to f_c', ε_c'. Beyond $0.6\varepsilon_c'$, the dilation ratio increases with increasing axial strain. At an axial strain of approximately $2\varepsilon_c'$, the dilation ratio appears to stop increasing. This limiting dilation ratio is referred to as η_u.
5. The limiting dilation ratio is inversely proportional to the level of confinement provided. It is noted that for all specimens tested, the limiting dilation ratio exceeded 0.5, indicating volumetric expansion of the concrete within the jacket.

Table 2
Summary of average experimental results

Plies (n)	f_{cmax} (MPa)	f_{cmax}/f_c'	ε_{cmax}	$\varepsilon_{cmax}/\varepsilon_c'$	ε_{cu}	ε_{tu}	$\eta_u = \varepsilon_{tu}/\varepsilon_{cu}$
0	$f_c' = 32.1$	1.00	$\varepsilon_c' = 0.0028$	1.00	0.0039	unstable at $\eta_u > 0.50$	
E-Glass							
1	36.8	1.15	0.0021	0.75	0.0044	unstable at $\eta_u > 0.50$	
2	36.6	1.14	0.0022	0.78	0.0040		
3	36.6	1.14	0.0023	0.81	0.0050	0.012	2.41
6	37.6	1.17	0.0031	1.10	0.0057	0.0103	1.81
9	46.7	1.46	0.0068	2.40	0.0068	0.0111	1.63
12	50.2	1.56	0.0082	2.89	0.0082	0.0109	1.32
15	60.0	1.87	0.0087	3.05	0.0087	0.0111	1.28
Carbon							
1	32.9	1.03	0.0024	0.85	0.0060	0.0103	1.72
2	35.8	1.12	0.0022	0.76	0.0086	0.0119	1.38
3	52.2	1.63	0.0138	4.86	0.0138	0.0155	1.12

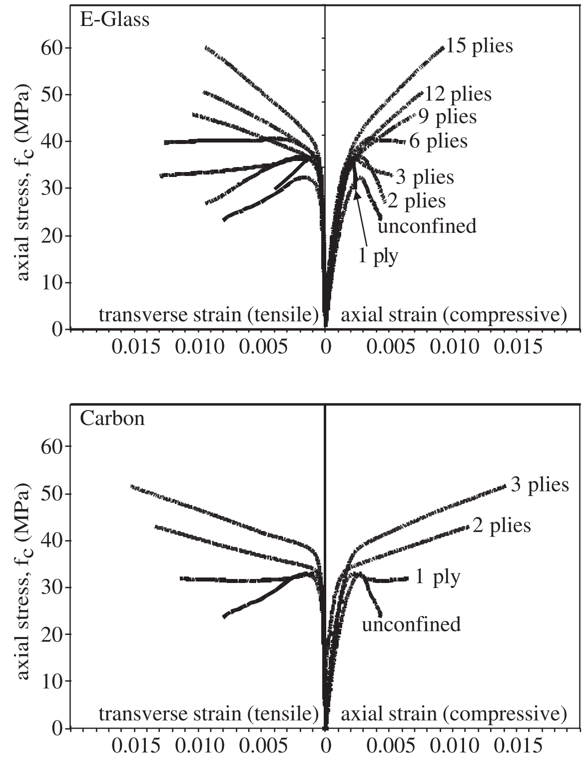

Fig. 4. Representative axial stress versus axial and transverse strain responses.

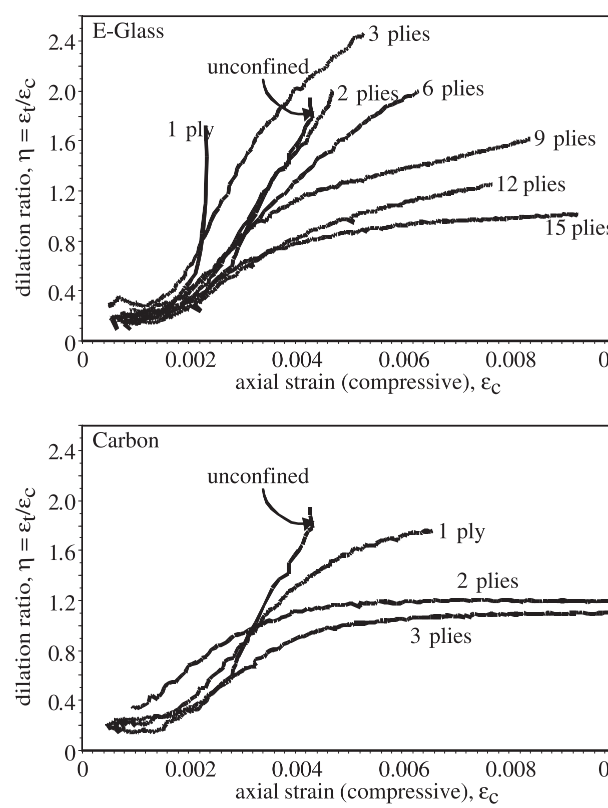

Fig. 5. Representative dilation versus axial strain relationships.

From Fig. 4, two distinct types of axial stress–strain behaviors can be seen. These depend on the stiffness of the confining material. These two behaviors and the transition between them are described in the following sections.

4.1. Lightly confined concrete

In the case of lightly confined one- and two-ply E-Glass-confined cylinders, the jackets did not fail at the peak axial load. A significant postpeak behavior is observed. This is because the jacket is not stiff enough to provide sufficient confining pressure at lower axial strains to increase the load carrying capacity of the concrete. To rupture the jacket, axial strain is increased until rupture strain of the jacket is achieved. The "confined concrete" at this point is "confined rubble." For lightly confined concrete, the limiting dilation ratio is not reached due to the limited strain capacity of the jacket.

4.2. Heavily confined concrete

In the case of heavily confined 12- and 15-ply E-Glass and 3-ply carbon-confined cylinders, the jackets are stiff enough to provide enough confining pressure to increase the load capacity resulting in larger dilation strains. When the confining material fails, the now overloaded unconfined concrete experiences a very brittle failure. In this case, no postpeak behavior is seen.

In the case of heavily confined concrete, an approximately bilinear stress–strain behavior is seen. In these cases, the dilation ratio is observed to increase to some limiting value after which it remains essentially constant. The ultimate axial stress and strain achieved is therefore related to the rupture strain of the confining material by the dilation ratio.

4.3. Moderately confined concrete

For moderately confined concrete, falling between the behaviors described above, a relatively smooth transition of response parameters between lightly and heavily confined concrete is observed. In these tests, this transition between responses appears at around the six-ply E-Glass-confined specimens.

5. Discussions

5.1. Maximum concrete stress

For comparison, Fig. 2 shows commonly used relationships between confining pressure, f_{con}, and maximum compressive strength, f_{cmax}, of confined concrete proposed by others [4–6,15,16]. Also shown in Fig. 2 is the data generated in this study. It is clear that the model proposed by Mirmiran and Shahawy [16] provides the best estimate of f_{cmax} from f_{con}.

$$f_{cmax} = f'_c + 4.269(f_{con})^{0.587} \text{ (MPa units)} \tag{1}$$

The values of f_{con} shown in Fig. 2 were derived from experimental data using the following relationship for cylindrical confinement:

$$f_{con} = \frac{4n\overline{E}_f}{D}\varepsilon_{tu} \tag{2}$$

where n = number of plies of FRP used; $\overline{E}_f$ = experimentally determined FRP material stiffness; D = diameter of the concrete cylinder; ε_{tu} = experimentally determined ultimate transverse strain in the concrete.

5.2. Confining material and "slackness"

From Table 2 it appears as though the confinement provided by one layer of carbon is approximately equivalent to that provided by three layers E-Glass. This ratio is consistent with that reported in Table 1 for jacket tensile moduli.

At similar levels of confinement (determined by f_{cmax}) the dilation ratio for the E-Glass specimens is greater than that for carbon specimens. This observation may be due to "slackness" in the glass confinement. The slackness may be envisioned as a gap between the concrete and the confining jacket. The confining jacket is not engaged until the transverse stain resulting from dilation closes this gap. Only at this point is confining pressure engaged.

In the case presented here, there is no gap, however, the behavior of the woven E-Glass fabric is similar to that of a gap. The longitudinal strands of a woven fabric are "kinked" as they pass over and under the transverse strands. In order to engage the tensile capacity of the longitudinal strands, they need to be "straightened." The stiffness of the confining material is negligible until the strands are straightened. Thus, confining pressure is also negligible until this point. For this reason, transverse strains measured on the exterior of the jacket are greater for a woven fabric. This is not an issue with the carbon fabric used, which is a unidirectional tow sheet.

The effect of "slackness" or an initial gap between the dilating concrete and the confining jacket are the subjects of the second part of this investigation [23].

5.3. Dilation ratio, η

Confining pressure is generated through transverse strain associated with the principal axial strain, which engages the confining material, causing confining pressure to be developed. The relationship between transverse strain, ε_t, and axial strain, ε_c, is given by:

$$\varepsilon_t = \eta\varepsilon_c \tag{3}$$

where η is the dilation ratio, determined as a function of the axial strain, ε_c, as discussed below.

The dilation ratio, η, is determined as a function of the ratio of principal axial strain in the concrete to axial strain at peak axial stress of the unconfined concrete, that is $\varepsilon_c/\varepsilon_c'$. This ratio was selected as it appears to allow convenient points at which the dilation behavior changes. Fig. 6 is a schematic representation of the experimentally determined dilation plots shown in Fig. 5. As can be seen from Figs. 5 and 6:

- At $\varepsilon_c/\varepsilon_c' = 0.6$, the dilation ratio begins to increase from its initial value, η_i; and,
- at $\varepsilon_c/\varepsilon_c' = 2$, the dilation ratio stops increasing and remains constant at its ultimate value, η_u.

Between these values of $\varepsilon_c/\varepsilon_c'$, a linear relationship between dilation ratio and $\varepsilon_c/\varepsilon_c'$ may be assumed. Thus, the relationship used to determine the dilation ratio, η, for a given axial strain, ε_c, is given as:

$$\begin{aligned} &\eta = \eta_i && \text{for } \varepsilon_c < 0.6\varepsilon_c' \\ &\eta = \left(\frac{\eta_u - \eta_i}{1.4\varepsilon_c'}\right)(\varepsilon_c - 0.6\varepsilon_c') + \eta_i && \text{for } 0.6\varepsilon_c' < \varepsilon_c < 2\varepsilon_c' \qquad (4) \\ &\eta = \eta_u && \text{for } \varepsilon_c > 2\varepsilon_c' \end{aligned}$$

In Eq. (4), the initial dilation ratio, η_i, is taken as Poisson's ratio for concrete. If very large amounts of confinement are present, a lower value may be appropriate [24]. This was not the case in the present study.

Finally, the transverse strain, ε_t, in Eq. (3) is limited by the rupture strain of the confining jacket, ε_{jr}, as shown by the heavy dashed line in Fig. 6. For lightly confined concrete, rupture of the confinement may occur prior to the ultimate dilation ratio being reached. This is shown schematically in Fig. 6 as the uppermost curve.

Fig. 7 shows the relationship between the limiting dilation ratio, η_u, and the confining jacket stiffness, $n\overline{E}_f$.

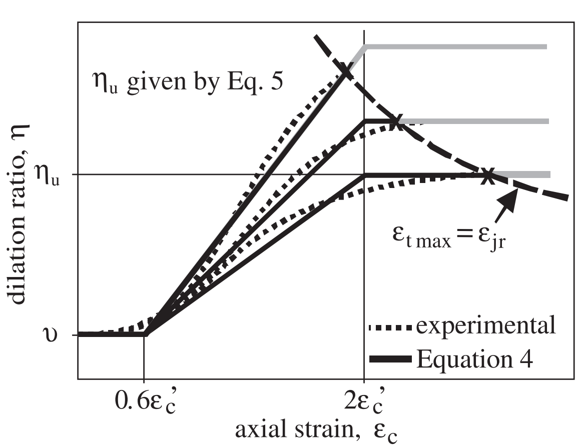

Fig. 6. Schematic representation and idealization of dilation behavior.

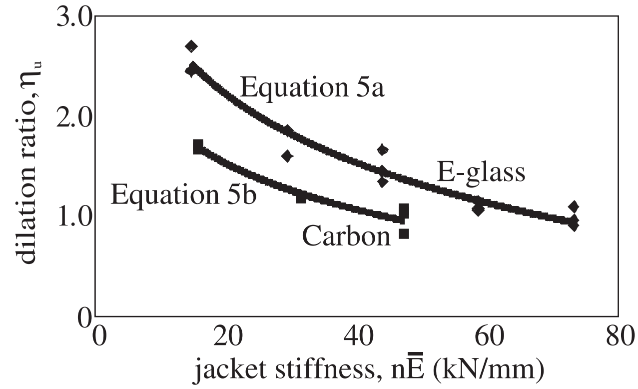

Fig. 7. Observed limiting dilation ratios versus jacket stiffness.

As can be seen from this figure there is a difference between E-Glass and carbon. Theoretically, there should not be any difference between the materials since the plot is normalized by $\overline{E}_f$. The observed difference is due to the "slackness" described previously.

The value of the limiting dilation ratio, η_u, is a function of the confinement provided. Eqs. (5a) and (5b) give the empirical relationships relating ultimate dilation ratio, η_u, to confinement stiffness, $n\overline{E}_f$, for the E-Glass and carbon materials, respectively:

$$\eta_u = -0.99\ln(n\overline{E}) + 12 \quad (R^2 = .95) \tag{5a}$$

$$\eta_u = -0.66\ln(n\overline{E}) + 8 \quad (R^2 = .95) \tag{5b}$$

Further investigation, beyond the scope of the present work, is necessary to establish a single relationship accounting for FRP material geometry ("slackness").

6. Summary and conclusions

The axial stress–strain behavior of concrete subject to variable confining pressure through the use of FRP jackets has been presented. Such jackets provide passive variable confinement. This confinement is engaged by the lateral expansion of the concrete associated with the applied axial compression. The following conclusions can be made from the experimental results obtained in this study:

1. In concrete confined with FRP jackets, maximum concrete stress, f_{cmax}, increases with an increase in the confinement used.
2. The strain corresponding to the maximum concrete stress, ε_{cmax}, increases with an increase in confinement used. This increase is greater than the increase in maximum concrete stress.

3. Axial concrete stiffness is not significantly affected by the presence of confinement.
4. As the level of confinement is increased, the axial stress–strain behavior of the concrete progresses from essentially parabolic (unconfined and low levels of confinement) to elastic–plastic having little postpeak stiffness (moderate confinement) to bilinear having significant postpeak stiffness (high levels of confinement).
5. The dilation ratio of axially loaded confined concrete varies with compressive strain. The observed initial dilation ratio is approximately equal to Poisson's ratio and remains essentially constant to an axial strain of about $0.6\varepsilon_c'$. Beyond this point, the dilation ratio increases with increasing axial strain. At an axial strain of approximately $2\varepsilon_c'$, the dilation ratio appears to stop increasing. This limiting dilation ratio is referred to as η_u.
6. The limiting dilation ratio is inversely proportional to the level of confinement provided.

7. Further research

Through the course of this research, the following have been identified as areas for further investigation.

1. A strain efficiency factor, relating in situ FRP jacket strains and the strains obtained from tensile coupon tests, has been previously described [19]. Experimental verification of this relationship is necessary.
2. The effect of confinement on larger-scale specimens and those having conventional internal reinforcement is required to calibrate the model and conclusions presented for larger specimens.
3. As discussed previously, slackness of the E-Glass material is believed to have affected the dilation behavior. Further research needs to be done to verify this. This may be accomplished by debonding the jacket and providing a gap between the jacket and the confined concrete. Furthermore, FRP materials having different weave geometries should be investigated. This is discussed in the companion paper [23].
4. FRP jackets have very high in-plane tensile stiffness but as they are typically quite thin, they have very small out-of-plane stiffness. Therefore, effective confining pressure is only generated where the jacket is engaged in tension. Unlike circular sections, rectilinear sections having external confinement do not experience uniform confining pressure from external confinement. Dilation of the concrete section results in significant confining pressure developed across the diagonals of rectangular sections. The jacket sides provide smaller levels of confinement since confining pressure at this location is engaged more by the flexural stiffness of the jacket. Further study needs to be done with rectangular cross-section specimens to investigate this effect. This is discussed in the companion paper [23].

Notation Used

D diameter of concrete cylinder
$\bar{E}_f$ tensile modulus of FRP material
$\bar{f}_{fr}$ strength of FRP material
f_{cmax} maximum strength of confined concrete, for unconfined specimens $f_{cmax} = f_c'$
f_c' unconfined concrete compressive strength
f_{con} confining pressure
n number of plies of FRP material
ε_{cmax} strain in confined concrete corresponding to f_{cmax}, for unconfined concrete $\varepsilon_{cmax} = \varepsilon_c'$
ε_{cu} ultimate axial strain of concrete (for heavily confined concrete $\varepsilon_{cu} = \varepsilon_{cmax}$)
ε_c' concrete compressive strain corresponding to f_c'
ε_{fr} rupture strain of FRP coupon
ε_{jr} in situ rupture strain of FRP jacket
ε_t transverse strain in concrete
η dilation ratio
η_i initial dilation ratio = Poisson's ratio
η_u ultimate or limiting dilation ratio of concrete

Acknowledgements

This research was partially funded by a USC Research and Productive Scholarship Award and by start-up funds available to Dr. Harries. The authors would like to acknowledge the assistance of Mr. Shawn Carey. Composite Structures Technology is acknowledged for their assistance with the lightweight FRP materials.

References

[1] S. Popovics, A numerical approach to the complete stress–strain curve of concrete, Cem. Concr. Res. 3 (5) (1973) 583–599.
[2] E. Thorenfeldt, A. Tomaszewicz, J.J. Jensen, Mechanical properties of high strength concrete and application in design, Proceedings of the Symposium on Utilization of High Strength Concrete, Tapir, Trondheim, 1987, pp. 149–159.
[3] M.P. Collins, Stress–strain relationships of high-strength concrete for use in structural design, paper presented at the April 1992 Meeting of the Network of Centres of Excellence on High Performance Concrete, Montréal, 1992, 20 pp.
[4] F.E. Richart, A. Brandtzaeg, R.L. Brown, A study of the failure of concrete under combined compressive stresses, Univ. Ill. Bull. XXVI (12), 105 pp.
[5] K. Newman, J.B. Newman, Failure theories and design criteria for plain concrete, structures, solid mechanics and engineering design, Proceedings of the Southampton 1969 Engineering Materials Conference, Part 2, 1971, pp. 963–995.
[6] D. Cusson, P. Paultre, Stress–strain model for confined high-strength concrete, ASCE J. Struct. Eng. 121 (3) (1985) 468–477.
[7] H.B. Kupfer, H.K. Hilsdorf, H. Rusch, Behavior of concrete under biaxial stresses, ACI J. 66 (8) (1969) 656–666.
[8] T.C.Y. Liu, A.H. Nilson, F.O. Slate, Stress–strain response and fracture of concrete in uniaxial and biaxial compression, ACI J. 69 (5) (1972) 191–295.
[9] D. Darwin, D.A.W. Pecknold, Non-linear biaxial stress–strain law for concrete, ASCE J. Eng. Mech. Div. 103 (EM2) (1977) 229–241.

[10] K.H. Gerstle, Simple formulation of biaxial concrete behavior, ACI J. 78 (1) (1981) 62–68.
[11] R. Park, D.C. Kent, R.A. Sampson, Reinforced concrete members with cyclic loading, ASCE J. Struct. Div. 98 (ST7) (1982) 1341–1360.
[12] R. Park, N.J.M. Priestley, D.G. Wayne, Ductility of square confined concrete columns, ASCE J. Struct. Div. 108 (ST4) (1982) 929–950.
[13] S.A. Sheikh, S.M. Uzumeri, Strength and ductility of tied concrete columns, ASCE J. Struct. Div. 106 (5) (1980) 1079–1102.
[14] J. Vallenas, V.V. Bertero, E.P. Popov, Concrete Confined by Rectangular Hoops Subject to Axial Load, EERC Report No. 77/13, University of California, Berkeley, 1977.
[15] J.B. Mander, N.J.M. Preistley, R. Park, Theoretical stress–strain model for confined concrete, ASCE J. Struct. Eng. 114 (8) (1988) 1804–1826.
[16] A. Mirmiran, M. Shahawy, Behavior of concrete columns confined by fiber composites, ASCE J. Struct. Eng. 123 (5) (1997) 583–590.
[17] W.F. Chen, Plasticity in Reinforced Concrete, McGraw Hill, New York, 1982.
[18] A.A. Elwi, D.W. Murray, A 3D hypoelastic concrete constitutive relationship, ASCE J. Eng. Mech. Div. 105 (4) (1979) 623–641.
[19] S. Pessiki, K.A. Harries, J. Kestner, R. Sause, J.M. Ricles, The axial behavior of concrete confined with fiber reinforced composite jackets, ASCE J. Compos. Constr. 5 (4) (2001) 237–245.
[20] K.A. Harries, G. Kharel, Behavior of variably confined concrete, ACI Mater. J. 99 (2) (2002) 180–189.
[21] G. Kharel, Behavior and Modeling of Variably Confined Concrete, MSc Thesis, Department of Civil and Environmental Engineering, University of South Carolina, 2001, 98 pp.
[22] ASTM C39-96, Standard Test Method for Compressive Strength of Cylindrical Concrete Specimens, ASTM, West Conshohocken, PA, 1996.
[23] K.A. Harries, S.A. Carey, Shape and "gap" effects on the behavior of variably confined concrete, Cem. Concr. Res. 33 (6) (2003) 881–890 (accepted for publication, companion paper).
[24] J. Kestner, K.A. Harries, S. Pessiki, R. Sause, J.M. Ricles, Rehabilitation of Reinforced Concrete Columns Using Fiber Reinforced Polymer Composite Jackets, Lehigh University, ATLSS Report No. 97-07, 1997, 196 pp.